# ETHzürich

ETH Library

# Predicting resilience of migratory birds to environmental change

**Journal Article**

**Author(s):**
Lisovski, Simeon; Hoye, Bethany J.; Conklin, Jesse R.; Battley, Phil F.; Fuller, Richard A.; Gosbell, Ken B.; Klaassen, Marcel; Lee, Chengfa Benjamin; Murray, Nicholas J.; Bauer, Silke

# Predicting resilience of migratory birds to environmental change

Simeon Lisovski[a,1] (ID), Bethany J. Hoye[b] (ID), Jesse R. Conklin[c] (ID), Phil F. Battley[d] (ID), Richard A. Fuller[e] (ID), Ken B. Gosbell[f] (ID), Marcel Klaassen[f,g] (ID), Chengfa Benjamin Lee[h,i] (ID), Nicholas J. Murray[j] (ID), and Silke Bauer[k,l,m,n] (ID)

The pace and scale of environmental change represent major challenges to many organisms. Animals that move long distances, such as migratory birds, are especially vulnerable to change since they need chains of intact habitat along their migratory routes. Estimating the resilience of such species to environmental changes assists in targeting conservation efforts. We developed a migration modeling framework to predict past (1960s), present (2010s), and future (2060s) optimal migration strategies across five shorebird species (Scolopacidae) within the East Asian-Australasian Flyway, which has seen major habitat deterioration and loss over the last century, and compared these predictions to empirical tracks from the present. Our model captured the migration strategies of the five species and identified the changes in migrations needed to respond to habitat deterioration and climate change. Notably, the larger species, with single or few major stopover sites, need to establish new migration routes and strategies, while smaller species can buffer habitat loss by redistributing their stopover areas to novel or less-used sites. Comparing model predictions with empirical tracks also indicates that larger species with the stronger need for adaptations continue to migrate closer to the optimal routes of the past, before habitat deterioration accelerated. Our study not only quantifies the vulnerability of species in the face of global change but also explicitly reveals the extent of adaptations required to sustain their migrations. This modeling framework provides a tool for conservation planning that can accommodate the future needs of migratory species.

global change biology | optimal migration | habitat deterioration | avian migration | stochastic dynamic programming

## Significance

Predicting the capacity of migratory animals to adjust to environmental change is a key challenge in ecology. We developed a modeling framework to predict migrations of several shorebird species, using past (1960s), present (2010s), and potential future (2060) conditions, in one of the world's most rapidly changing flyway—the East Asian-Australasian Flyway. By comparing model predictions with empirical tracks, we show how much migrations need to change and how the required changes differ markedly among species. Overall, larger species require more fundamental changes, such as using entirely different sites and routes, to maintain optimal strategies, whereas smaller species need less-profound adjustments. Our framework provides a powerful tool to identify required adaptations in migratory behavior due to multiple concurrent environmental changes.

Environmental change threatens biodiversity worldwide (1). Migratory animals are especially vulnerable since they rely on intact chains of resources along their migration routes (2). While some migrants have responded by adjusting their migration routes and schedules, the responses have typically been insufficient to keep pace with recent environmental change (3, 4). Migrants increasingly encounter multiple and often independent threats across sites they visit during their journeys (5, 6). Among these changes, climate change is altering the optimal timing of migration (7, 8), leading to phenological mismatches between migrants and their food sources (9, 10). Habitat deterioration, on the other hand, threatens the integrity of the network of sites that connect breeding and nonbreeding locations, notably if it extends into considerable or complete loss of habitat. Even if only occupied for a short period of time, specific staging sites within a migration network can be crucial to sustaining overall migration flow and hence the persistence of entire populations (2). Consequently, even low levels of habitat deterioration at critical sites can lead to rapid declines or even extinction when alternative sites are lacking, particularly when migrants possess inadequate adaptive capacity to compensate for these changes (11, 12). Thus, predicting the capacity of migrants to adaptively adjust to environmental change is one of the key challenges in ecology (13). Until recently, limited possibilities to track individual migration behavior have hampered understanding of whether migrants have responded to past and ongoing changes, whether these responses are sufficient, and what type and degree of response is needed to persist under future environmental change scenarios.

The East Asian-Australasian Flyway has seen profound habitat degradation and loss due to pollution, overexploitation, and land reclamation over the last six decades (14). Millions of shorebirds migrate along this flyway coannually and rely on intertidal mudflats along the coast for resting and refueling. In the Yellow Sea region, habitat deterioration has been most intense with an estimated loss of intertidal mudflats of over 50% (15), a number which only includes the shrinking and complete loss of sites but not the concurrent reduction in the quality of remaining habitats and sites. This particular region, however, hosts a large proportion of the flyway's migratory shorebirds during migration (15, 16). The rapid declines of many shorebird species and populations are a likely consequence of these changes (17–19), and there is concern that with the loss of these and other migrants across the

globe, a major component of biodiversity will be lost along with their important functional roles in ecosystems worldwide (20, 21).

Migratory birds in general, and shorebirds in particular, are declining across most of the world's major flyways (e.g., refs. 13 and 22). Yet, even within the East Asian-Australasian Flyway, there is great variation in the magnitude of declines (18): Some species are declining by up to 11% per year (e.g., Curlew Sandpiper, *Calidris ferruginea*), while others seem relatively stable (e.g., Red-necked Stint, *Calidris ruficollis*). Although the exact reasons for these varying declines remain unclear, they are presumably driven by a combination of the varying speed and magnitude of environmental changes in different sites interacting with each species' intrinsic migration strategy (12, 23, 24). Migration strategies are at least partly dependent on body size (25), which sets physiological capacities, including factors such as how far a bird can fly in a single bout, the amount of body reserves it can accumulate, and the energetic cost of flight. Migration strategies mainly differ in the number of intermediate stopover sites used and the distances covered between them. Environmental changes may affect species with different migration strategies differently. For instance, if a migrant with a single stopover site and long migration bouts faces habitat deterioration at its only stopover site, it must either change migration strategy or it will go extinct (26), whereas the loss of one stopover site might only require slight adjustments to the overall migration strategy if that site is part of a well-connected network of many stopover sites (23).

Here, we develop a modeling framework to predict the optimal migration strategies of shorebirds. We focus on both ecological and species-specific features, including body size and physiological capacity, and relate these to observed changes in environmental conditions across the East Asian-Australasian Flyway. For specific populations of five closely related shorebird species (Scolopacidae) with contrasting body sizes, we predict optimal historical (1960s), present (2010s), and future (2060s) migration strategies and compare model predictions with empirical tracking data (n = 61) collected between 2013

and 2019. Specifically, we test the hypotheses that a) species with smaller body sizes require more stopover sites distributed along the flyway and can thereby buffer adverse changes at specific sites, and b) the observed migrations of smaller species today are closer to their predicted optimal migrations, whereas larger species require more significant changes in their migrations and are more likely to display suboptimal journeys given the recent period of rapid environmental change. In addition, we identify the relative importance of stopover regions across the flyway and predict how this may shift to novel areas and require the establishment of novel stopover sites under future environmental changes.

## Modeling Optimal Migration

We developed a state-dependent dynamic migration model to calculate the fitness-maximizing movement decisions of a migratory bird (27–29) on its (northward) migration from nonbreeding to breeding sites. We particularly focused on spring migration because of its explicit relevance for individual fitness (e.g., ref. 30). In each time-step, a bird can choose between remaining and foraging on its present site or migrating to one of the next sites. Decisions depend on body stores, time of the year, and expected conditions at present and subsequent sites. The model was parameterized for specific populations of five closely related shorebird species (Fig. 1) for which empirical tracks (n = 61) of their migrations along the East-Asian Australasian flyway exist: Bar-tailed Godwit *Limosa lapponica baueri*, Great Knot *Calidris tenuirostris*, Red Knot *Calidris canutus* (5 *rogersi* and 1 *piersmai*), Curlew Sandpiper, and Red-necked Stint. We calculated the optimal, i.e., fitness-maximizing, decisions, which included trade-offs between gaining energy and avoiding predation, and also weighed the benefits (or costs) of being closer to the breeding grounds against the benefits (or costs) of staying at the present site (for details on how optimal decisions are calculated, see *Materials and Methods* and *SI Appendix*, section S1).
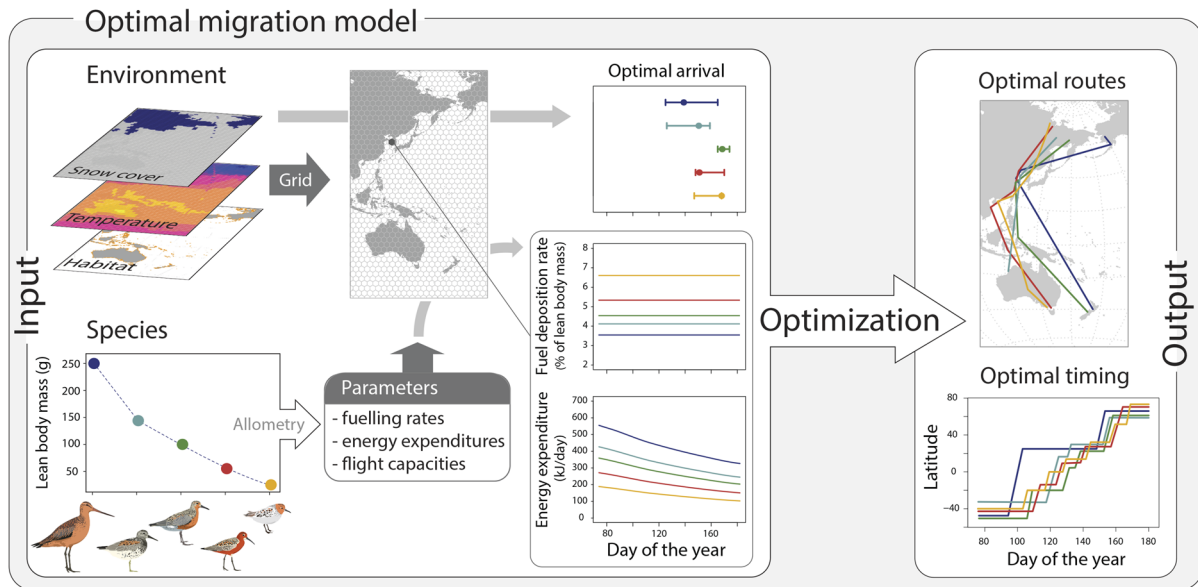


**Fig. 1.** Major input data and parameter calculations of the model, leading to predictions of optimal routes and migration timing in shorebirds along the East Asian-Australasian Flyway. Remotely sensed data on intertidal mudflat extent, snow cover, and modeled surface temperature were summarized into daily grids spanning the flyway. Species-specific parameters, such as maximum fueling rates, temperature-dependent energy expenditure, and flight capacities, were calculated using established allometric relationships and the species' lean body mass. The spatially explicit datasets were then combined with the species parameters to derive grid-based optimal arrival dates (figure shows optimal arrival dates for locations of individual-specific breeding sites), fueling rates, and energy expenditure over time. The state-dependent optimization routine produces decision matrices (probability of moving to any site on a given day and for any possible body condition) that are used to predict optimal migration routes and timing. Bird illustrations by José A. Senciales, courtesy of Conservation of Arctic Flora and Fauna (CAFF).

The most relevant model parameters define species-specific phys-iological identities such as subsistence energy (temperature-dependent energy expenditure), maximal fueling rates, and flight costs. The East Asian-Australasian Flyway was divided into a hexagonal grid (diameter of 400 km and area of 138.564 km$^2$). Environmental conditions in each cell were defined for scenarios of past (1960s), current (2010s), and predicted future conditions (2060s). We used a set of three variables—daily temperature, intertidal mudflat extent, and snowmelt date—assuming that i) ambient temperatures influ-ence energy expenditure, ii) intertidal mudflat extent characterizes food availability and thus foraging options, and iii) snowmelt date determines optimal arrival time at the breeding grounds. Their spe-cific values were extracted from remote sensing and climate reanal-ysis modeling products for past and present conditions as well as for future temperature projections. Potential habitat availability and optimal arrival timing for future scenarios were extrapolated from the trend and inferred by temperature projections, respectively (for details, see *Materials and Methods* and *SI Appendix*, section S2).

For each empirical track, with its specific major nonbreeding site and breeding site combination, we simulated 200 species-specific optimal migration trajectories for each period (1960s, 2010s, and 2060s). From all modeled tracks, as well as from the empirical tracking results, we extracted values characterizing migration strat-egies: migration duration as the period from the departure in spring to the arrival at the breeding site and migration distance as the distance traveled from major nonbreeding site to the breeding site. In addition, we grouped the number of stopover sites of empirical tracks based on the spatial grid of the model to allow comparison between model prediction and empirical tracks. The duration of the stopover per site was also used to derive individual and species-specific migration strategies.

## Results

**Empirical Tracks.** Individual geolocator tracks indicate distinct species-specific spring migration strategies (Fig. 2, *Left* panel) in terms of distances, number of stopover sites, and relative time spent on each site. The largest species, the Bar-tailed Godwit [250 g lean body mass (lbm)], migrated the longest distances (16,200 ± 550 km), employing the extreme "jump" strategy with only one major stopover site in the Yellow Sea where individuals spent on average 88.2% (95th percentile; 71.8 to 100%) of the entire migration
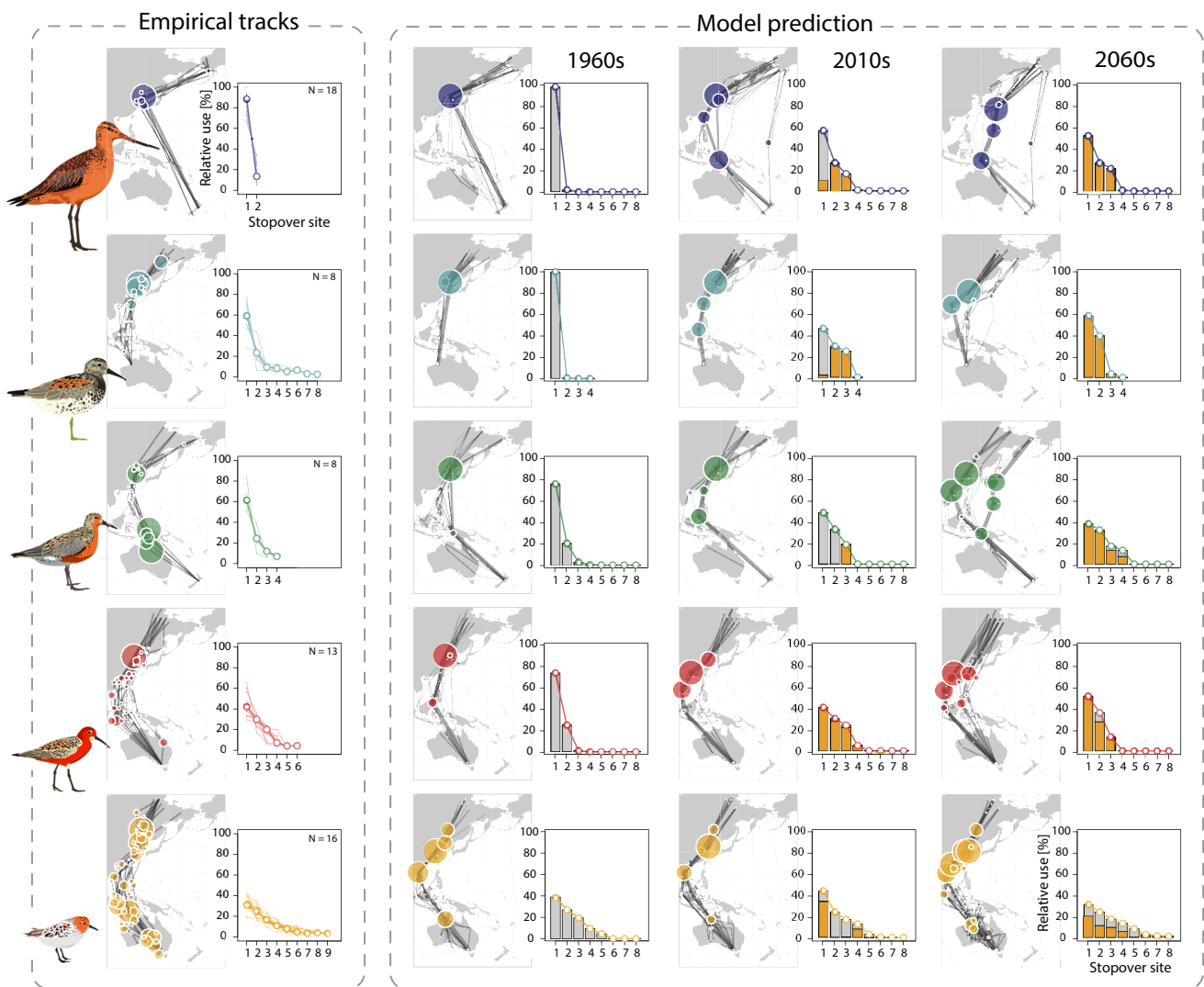


**Fig. 2.** Empirical tracking results for the five species (*Left* panels: Bar-tailed Godwit, Great Knot, Red Knot, Curlew Sandpiper, and Red-necked Stint) and model predictions for the past (1960s), the present (2010s), and future (2060s) periods. The colored circles indicate stopover sites with the size showing the relative time spent during the prebreeding migration period and across all individuals of the species. The *Right* bar-plot panels for each modeled prediction show the general migration strategy of relative site use. The *x* axis indicate the number of stopover sites ordered by the time spent on this site in relation to the entire migration duration. Orange color illustrates the percentage of new sites in relation to the 1960s model prediction. Bird illustrations by José A. Senciales, courtesy of CAFF.

duration. Only a small fraction of time (11%, 95th percentile; 0 to 30.7%) was spent on a second site, close to the major stopover site. Great Knots (144 g lbm) and Red Knots (105 g lbm) made use of several stopover sites (range: 4 to 8 sites) of which one or two sites were used for a much longer period of time compared to the other sites [58.2% (34.8 to 76.4) and 63.5% (52.6 to 81.9) of the entire migration duration, respectively]. The major stopover site of Great Knots was in the Yellow Sea region, used for 78.8% (55.4 to 94.5) of total migration duration, Red Knots extensively used shorelines in northern Australia (e.g., Gulf of Carpentaria) and southern Indonesia [61.3% (52.6 to 81.9) of total migration duration]. The two smaller species, the Curlew Sandpiper (55 g lbm) and the Red-necked Stint (23 g lbm), generally used more stopover sites (range of 3 to 6 and 4 to 10, respectively) with a larger spatial spread and tended to spend time on those sites more evenly (Fig. 2).

**Model Predictions and Comparisons.** The model predicted different migration strategies for the species, which generally also changed markedly over time, with the exception of Red-necked Stint (Fig. 2). Comparing empirical tracks with model predictions showed apparent similarity between empirical tracks and present-day scenario (2010s) predictions for the two smaller species, while for the three larger species there was a better apparent similarity with the predictions for the past scenario (1960s) (Fig. 2). This was corroborated by comparing the distribution of time spent at stopover sites between model predictions for the three different time periods and the empirical tracks (Fig. 3A). In the three larger species, the similarity was higher for predictions under past environmental conditions (1960s) (with r-squares of $r^2 = 1$, $r^2 = 0.96$, and $r^2 = 0.98$ in Bar-tailed Godwits, Great Knots, and Red Knots, respectively). In Curlew Sandpipers, the present and future scenarios had a higher

similarity ($r^2 = 0.99$, $0.98$) compared to the past scenario ($r^2 = 0.88$), and similarities did not differ between past and present predictions in Red-necked Stints ($r^2 = 0.97$ to $0.99$).

We quantified the necessary adaptations to maintain optimal migration strategies by comparing the predictions for the present (2010s) and future (2060s) scenarios with those for the past (1960s) scenario (Fig. 3 B, Left). Great Knots required the largest adaptations to remain within the optimal scope ($r^2 = 0.26$; values between 0 and 1 indicate the strength of the discrepancy between migration strategies in the 1960s to the respective period). Curlew Sandpiper ($r^2 = 0.17$) and Bar-tailed Godwit ($r^2 = 0.12$) also required a substantial adaptation, followed by Red Knots ($r^2 = 0.1$), whereas Red-necked Stints ($r^2 = 0.01$) did not need major changes to their migration strategy. In the comparison between past conditions and future scenarios, a strong correlation with body size was apparent, suggesting that the need to adapt would be largest in the three larger-bodied bodies species (Bar-tailed Godwits $r^2 = 0.16$, Great Knot $r^2 = 0.22$, Red Knot $r^2 = 0.18$) and considerably less in Curlew Sandpiper ($r^2 = 0.07$) and Red-necked Stint ($r^2 = 0.03$).

Model predictions also suggested a major change in the use and importance of sites between the different time periods (Fig. 3 B, Right). Comparing the present-day (2010s) simulation with the past simulation showed that the percentage of time spent in novel sites, i.e., sites not used before, is highest in Curlew Sandpiper (95.4%), intermediate in Bar-tailed Godwits (52.8%), Great Knots (54.7%), Red-necked Stints (43.0%), and lowest in Red Knots (19.6%). A strong body size relationship was found in the changes from the past to the future conditions, with the largest species stopping at sites that were almost never used in the 1960s simulation (99.9% in Bar-tailed Godwits, and 100% in Great Knot). High proportions of time spent in new sites were also found in Red Knot (88.9%) and Curlew Sandpiper (91.1%), while this was considerably lower in Red-necked Stints (52.1%).

In all species except for the Red-necked Stint, predicted migration durations increased over time (Fig. 4; relative increase from past to future predictions, Bar-tailed Godwit 159%, Great Knot 185%, Red Knot 170%, Curlew Sandpiper 119%, Red-necked Stint 93%). In Curlew Sandpipers, the predicted migration duration was longest under present conditions (165% of past optimal migration). The predicted longer migration duration is a result of individuals leaving the wintering site considerably earlier (most pronounced differences between the past and the present scenarios) while also arriving slightly earlier on the breeding sites (due to earlier optimal arrival window in northern latitudes due to climate change: See details in *SI Appendix*).

The relative time spent at different latitudes changed across the three model predictions. Under past conditions (1960s), most individuals relied on the Yellow Sea region and notably Bohai Sea (~37 to 41 °N). This reliance on the Yellow Sea changed already for present (2010s) and even more so for future (2060s) conditions, under which birds increasingly use alternative locations that lie more southerly (20 to 33 °N and near the equator) and are more dispersed.

## Discussion

We have shown that simple body size and related allometric relationships can explain fundamental differences in migration strategy among species and how environmental change might differentially affect them. Indeed, morphology constrains the movement and dispersal of animals and can often explain bird and mammal responses to landscape structure (23, 31–33). Our model applies this concept to long-distance migration and demonstrates that general migration strategies, including timing and routes, can be predicted based on body size.
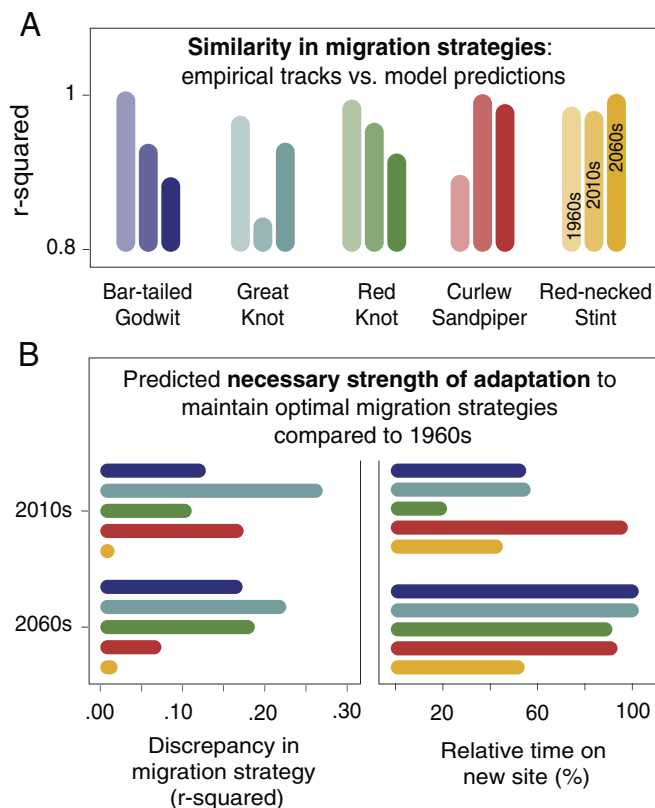


**Fig. 3.** Similarity of empirical tracks and predicted migration strategies (*A*) and predicted necessary strength of adaptation to migrate within the optimal range (*B*: relative site use and stopover at previously unused sites) in comparison to the 1960s scenario.
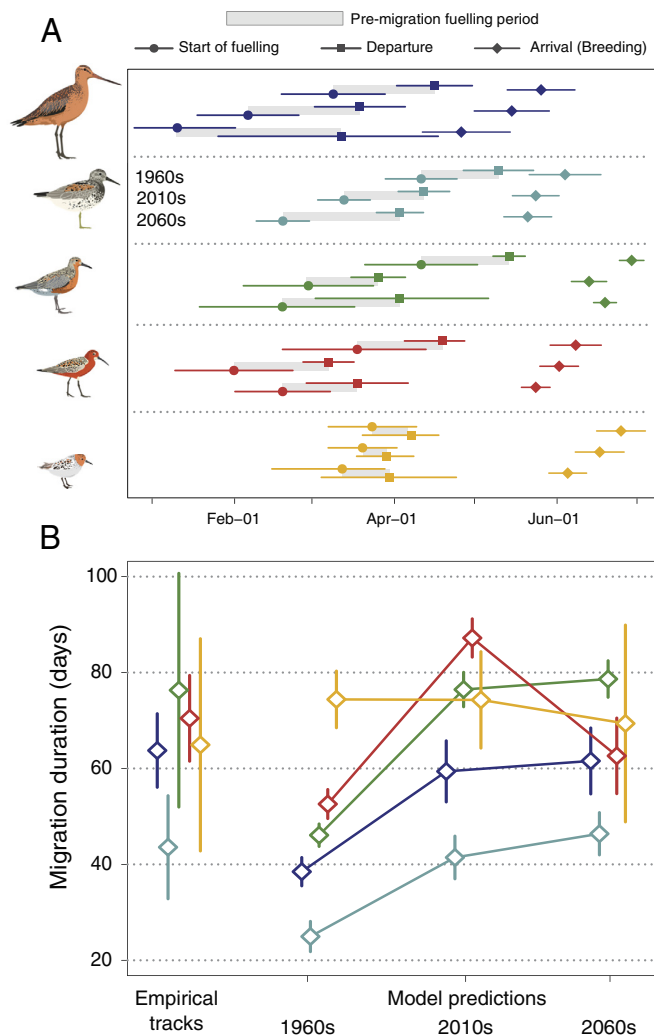
**Fig. 4.** Predicted changes in general migration phenology (*A*) and migration duration (*B*) for the five modeled shorebird species. The *Top* panel includes the timing of key migration events including the start of fueling on the wintering site (circle), the departure from the wintering site (square), and the arrival on the breeding site (diamond) for the three predicted time scenarios (1960s, 2010s, and 2060s). Gray rectangles indicate premigratory fueling periods. To be able to compare model predictions and empirical tracks, migration duration in *B*) is defined as the period between departure from the wintering site and arrival on the breeding site. Bird illustrations by José A. Sencianes, courtesy of CAFF.

A striking difference in migration strategies across species was the continuum of "hop, skip and jump" strategies (34), ranging from frequent stops in the small-bodied Red-necked Stint, through to extreme jump strategies in the much larger Bar-tailed Godwit that covers the distance from New Zealand to Alaska with a single major refueling stop (Fig. 2). The variation in migration strategy across this gradient therefore seems fundamental in influencing the resilience of species and populations to environmental change (e.g., ref. 23).

Within the East Asian-Australasian Flyway, the Yellow Sea region represents one of the most rapidly changing coastal environments on earth, with substantial decline of intertidal habitat (15) and concomitant pressure on the remaining areas (14). For shorebirds, and notably species belonging to the family Scolopacidae, the Yellow Sea with its vast extent of intertidal mudflats, rich food resources, and strategic location between the southern bounds of the flyway and the northern breeding sites, has shaped the evolution of migration strategies. As a result, we find some of the most stunning migrations at the "capital" end of the

"migratory capital-income continuum" (35), where larger-bodied species (e.g., Red Knot, Great Knot, and notably Bar-tailed Godwit) can achieve long-distance migrations of over 15,000 km with a single major refueling stop in the Yellow Sea (Fig. 2; refs. 36–38). These species at the capital extreme, which have each developed an advantageous strategy relying on strong environmental predictability, may now be trapped in their migratory niche (26, 35). Indeed, our model predicts that the migrations of these species would require the greatest changes to remain adaptive in the face of the ongoing environmental changes. In particular, Bar-tailed Godwit, and to a lesser extent Great and Red Knot, would require a shift toward a more "skipping" and "income" strategy, exploiting a higher number of sites (for shorter periods) along the flyway to compensate for deteriorating conditions on their historically established major fueling sites in the Yellow Sea (and notably Bohai Bay: ref. 4). However, as noted earlier, migrants making only very few refueling stops (i.e., near-capital migrants) tend to be highly faithful to their favored sites, maneuvering themselves into an ecological trap in which they fail to identify newly available, better-quality sites and stick to old sites and routes. Our model predictions indeed illustrate that the larger-bodied species still migrate in a fashion, notably with respect to the routes, that was optimal under the environmental conditions of the 1960s and have apparently scarcely modified their strategy to fit current conditions (3). In contrast, the much smaller Red-necked Stint requires no or only small changes in migration strategies to cope optimally with the changing environment. In this species' case, only a slight spatial shift in the time spent away from the sites that experienced the largest habitat deterioration might suffice to buffer these changes (Figs. 3 and 4).

Many migratory animals shift the timing of migration, e.g., to adapt to earlier springs (e.g., refs. 7 and 39), but potentially also to buffer changes in conditions en route (e.g., refs. 4 and 40), even though these adaptations in timing often seem weak or inadequate (3). Our model predictions suggest that significant phenological changes are required across species to adaptively respond to habitat deterioration and earlier springs, allowing for longer stopover durations for refueling en route and ensuring optimal arrival at the breeding grounds (Fig. 3A). With our parameterization of the environment, all species, except the Red-necked Stint could cover the migration distance in significantly shorter time periods in the past than nowadays. The small-sized Red-necked Stint seems to profit from higher temperatures and lower energy expenditure in the future scenario, allowing a shorter migration duration. As the currently observed migration durations match the model predictions for the current conditions, their timing might have adapted with earlier departure over the last decades. Indeed, a recent study showed that Bar-tailed Godwits have advanced their departures by around 0.5 d per year over the last decade (4). However, this earlier spring departure did not result in a significantly earlier arrival at the breeding grounds. Instead, this extra time was spent for longer stopovers on the major refueling sites in the Yellow Sea—a change that was also predicted by the model and indicative of the strong selection pressure to adapt to the deteriorating conditions (see also ref. 41).

Migratory birds are considered to be relatively consistent in both timing and routes (42), but both observational and experimental studies show that at least timing is often more flexible, especially in response to environmental changes (39, 43). In addition, evolutionary responses can play a significant role in changing stopover site locations and phenology through the recruitment of young individuals with alternative routes (44, 45) and earlier migration timing (46). However, given the unprecedented rate of changes in crucial habitats in this flyway and in the phenology of

Arctic breeding grounds [e.g., snowmelt timing (30, 47)], it is doubtful whether phenotypic plasticity and individual adaptations are sufficient to keep up with the rapid changes. The smaller-sized species might have another advantage here—due to their shorter generation times, intergenerational adaptations will take effect faster compared to the larger, longer-lived species (48, 49).

Our modeling approach highlights the potential of a predictive framework to integrate multiple concurrent changes and their complex interactions with species' behavior over large spatial scales. In running such models over past and potential future scenarios, they can provide insights across spatial and temporal scales and identify nonintuitive, complex responses and patterns. Our modeling approach focused on the flyway scale and on predictions in relation to environmental changes. Although we deliberately left out specific ecological characteristics that differ between species and sites, such as foraging preferences and prey availability, the model adequately captured the general broader migration behavior of the species. However, some discrepancies between empirical tracks and model predictions, e.g., major differences in stopover sites in the Red Knot (Fig. 2), may indicate regions that are not well parameterized with our large-scale approach and may warrant closer investigations. With more detailed and fine-scaled information on species and environments, this model framework can be adapted to also tackle important questions on habitat choice and regional changes in migration patterns. By running scenarios of change and/or planned habitat alterations, such models may also assist in identifying efficient conservation and management measures and where and when in the flyway they would be most beneficial (50).

## Materials and Methods

**Empirical Tracking Data.** Northward migration routes from 61 individuals (Table 1) of five closely related shorebird species (Bar-tailed Godwit; n = 18, Great Knot; n = 8, Red Knot; n = 6, Curlew Sandpiper; n = 14, Red-necked Stint; n = 16) were derived from light-level geolocators, deployed and recaptured on the wintering sites in Australia and New Zealand. Migration routes were derived from published datasets (Table 1 and refs. 36 and 51–54). Locations were estimated from light recordings using the R packages SGAT (Great Knot, Curlew Sandpiper, Red-necked Stint) and FLightR (Bar-tailed Godwit, Red Knot) following standardized protocols (55). Both packages yield the most likely tracks with error estimates and include a movement model and a spatial mask. Due to the distinct behavior between movements and distant stationary periods, location estimates are considered relatively precise and comparable between the two methods (55, 56). To allow comparison with the modeling results, the location estimates of stationary periods (stopover/resting sites) during northward migration were assigned to the hexagonal grid cells of the modeling framework (see model description). For each species, the cumulative time spent within each cell and the sum of movements between cells were used to create species-specific networks (Fig. 2). Migration distance and duration were calculated for each individual, as the distance and duration of the estimated track from the wintering to the breeding sites, respectively (Table 1). The general migration strategy of

species was characterized by calculating the relative time individuals spent at each stopover site and summarizing it for the population.

**State-dependent Dynamic Optimization Model.** We developed a state-dependent dynamic optimization model to calculate the behavioral decisions that maximize fitness during northward migration. In addition to the general model description section above, we here outline additional relevant model characteristics but reduce redundancy to earlier publications that have used the same general modeling framework by referring the reader to the detailed model descriptions (27, 28, 57, 58). The model requires parameters to define species-specific physiological identities and environmental conditions.

**Environmental Conditions.** The migration period was divided into whole days, and the spatial extent of the East Asian-Australasian Flyway was divided into a hexagonal grid with a cell size (diameter) of 400 km. NCEP-NCAR Reanalysis 1 daily surface temperature data on a 2.5 × 2.5 degree resolution were downloaded for the periods from 1960 to 1970 and 2010 to 2020 from the NOAA data repository (59), and for the future 2060 to 2070, the "middle of the road" 1 to 2.6 (SSP2) degree temperature increase projection was downloaded from the Copernicus Climate Data Store (CMIP6 SSP1-2.6 AWI-CM-1-1-MR; ref. 60). Data were extracted for each grid cell, and the median per day and the three time periods were used to describe the daily temperature across the migration period for past (1960 to 1970), present (2010 to 2020), and future (2060 to 2070) conditions. The mean temperature across grid cells included in the model and for the northward migration period increased from 14.8 °C in the past, to 15.3 °C in the present, and 17.6 °C in the future scenario.

Several datasets were used to define the quality and thereby daily rates of energy intake and expenditure for each grid cell, that is ultimately linked with species-specific fueling. First, the present extent of intertidal mudflats on a 30 × 30 m resolution was processed and downloaded via Google Earth Engine using the dataset published by Murray et al. (61). To avoid cutting mudflat areas by the border of grid-cells (and underestimating the true extent of the mudflats), the extended area around each grid cell (400 km radius from the center of each grid cell) was taken to define the km² of mudflats for each grid cell. The buffer also accounts for the potential movements of birds during stopover periods and provides a more realistic relative quality measure for the respective region. A polygonized historic dataset on the intertidal mudflat extent for the Yellow Sea Region and the entire Chinese coastline was used to define the past (1960s) habitat availability for all cells represented in this dataset (15). For all other cells, we assumed that no change in mudflat extent occurred. In addition to intertidal mudflats, a third of the area of mangrove forests [not part of the Murray et al. (61) dataset] growing in intertidal areas that partly provide resting and fueling habitat for migrating shorebirds, was added to the mudflat extent of each grid cell. The Global Distribution of Mangroves USGS v1.3 in km² units was downloaded from the UNEP-WCMC repository (62). Lakes in Australia, China, and Russia are known to provide important fueling and staging sites for shorebirds during migration (63). Each cell without any mangrove or intertidal mudflat extent but with overlap of a lake with larger than 1,500 km² (n = 28, 90th percentile of lakes within the flyway, based in Natural Earth 10 m Lake Dataset the free vector and raster map data @naturalearthdata.com) was flagged. For each grid cell that lies in the estimated breeding site of individuals (as derived from the empirical tracks), the snowmelt timing for past (1960s) and present (2010s) conditions was defined using the NOAA Northern Hemisphere Snow Cover Extent daily dataset (v01r01) with an approx. 250 km spatial resolution (64). Snowmelt timing was calculated

**Table 1. Empirically tracked species, location of tracking device deployment, year of tracking, number of collected tracks, individual migration distances (flown distance), and reference of published datasets**

| | Deployment | Year | Tracks | Distance (km) | Duration (d) | Ref |
|---|---|---|---|---|---|---|
| Bar-tailed Godwit | New Zealand | 2013–14 | 18 | 16,210 (±550) | 64 (±8) | (51) |
| Great Knot | Australia | 2013 | 8 | 9,920 (±465) | 44 (±11) | (36) |
| Red Knot | New Zealand | 2013 | 6 | 12,504 (±2,561) | 77 (±25) | (52) |
| Curlew Sandpiper | Australia | 2018–19 | 13 | 15,775 (±905) | 71 (±9) | (53) |
| Red-necked Stint | Australia | 2016–19 | 16 | 14,707 (±1,019)* | 65 (±22) | (54) |

Mean values with SD are provided.
*In a subset of Red necked Stints, the breeding sites could not be estimated and were set to the center of known breeding range (104°4′E and 72°80′N).

using a double sigmoidal fit for snow cover values (between 0 and 1) across the day of the year and applying a 0.75 threshold in spring, pooling data from 1960 to 1970 as well as 2010 to 2020. Due to the lack of snow cover projections, future (2060s) timing of snowmelt was set as the date when the cell-specific temperature projection surpasses the median value of the temperature that has been recorded at snowmelt timing in the 1950s and 2010s scenario (see *SI Appendix* for more details). Future habitat availability was extrapolated based on the trends between past and present conditions.

**Species Parameterization.** The relevant species-specific parameters were defined using established allometric relationships adjusted for shorebird taxa. For these, lean and maximum body masses (Table 2) provide the basis and were extracted from refs. 64 and 65. Based on empirically measured daily metabolizable energy intake (DME) and the daily energy expenditure (DEE) for birds of different body mass, a theoretical relationship was established to define maximum fat deposition rates (FDRmax) in relation to body mass (66). Comparison with empirical data summarized in ref. 67 shows that this relationship captures species differences well but slightly underestimates maximum fat deposition rates (likely because empirical data were collected at different sites with different underlying food quality). Thus, in our modeling, we multiplied the maximum fat deposition rates of the sites with their mudflat size scaled between 0.5 and 1.5 (cells with major lakes received the value of 1). The scaling results in low (50% of the estimated FDRmax) possible fuel deposition rates (FDR) for sites with at least some intertidal or/and mangrove habitat. Furthermore, only 2% of the largest sites in the past scenario exceed the 1 × FDRmax, which corresponds well with the proportion (2.2%) of empirical measurements that exceeds the established FDR relationship with lean body mass (see *SI Appendix* for more details).

Animals always expend energy, even when they are inactive. BMR is the energy expenditure of a nonproductive, postabsorbtive animal resting in thermoneutrality during the circadian rest phase (68). In our modeling framework, BMR is implicitly incorporated with the estimate of energy expenditure that also includes the costs of thermoregulation. Based on ref. 68, the relationship between BMR and body weight of shorebirds is best described by the allometric relation $BMR[Watts] = 5.06 \times BW[kg]^{0.704}$. Below thermoneutrality, metabolic rate increases linearly with decreasing air temperature. The extra temperature-dependent daily energy expenditure was calculated using established allometric relationships of conductivity (Watts) and critical lower temperature (°C) as well as transfer functions to derive kJ/day values (ref. 68, see *SI Appendix* for details).

Flight speed slightly differs across species and marginally increases with body mass. Given the small differences and the large variation between empirical measurements (69), we used a median air speed of 16.7 m/s for all five species. Maximum flight range was extracted from the geolocator tracking data (entire migration period) showing that experimental estimates of maximum flight ranges (e.g., from Red Knots in a wind tunnel, ref. 70) are slightly lower and that potential wind support might lead to larger distances. See Table 2 for most important species parameters in the models, and *SI Appendix* for more details.

**Optimization Routine.** A model bird was characterized by body reserves and location on a particular day. Body reserves, $x$, could vary between 0, when the bird reached a minimum body mass and was assumed to die of starvation, and $xmax = 100$ where the maximum fuel load was reached. The model calculates the fitness-maximizing series of daily decisions, i.e., whether to stay and forage on its present site or migrate to one of the next sites. Decisions depend on body stores, time of the year, and expected conditions on present and subsequent sites and included trade-offs between gaining energy, avoiding predation, and considering the benefits (or costs) of being closer to the breeding grounds against the benefits (or costs) of staying at the present site. If staying on the present site, a bird requires energy, for maintaining its metabolism and may choose to forage with a certain intensity. If gain from foraging exceeds expenditure, the bird increases, and otherwise depletes, its energy reserves. Since there might be stochastic differences in individual foraging success, we modeled the gain rate at a specific site as a discrete random variable and the probability of achieving a particular gain. Stochastic differences in foraging success imply that a bird might experience (a series of) "bad luck" in foraging, which elevate starvation risk when reserves are insufficient. Therefore, accounting for such stochasticity will often yield a higher "best" foraging intensity (see below) than under deterministic foraging success (71).

A bird may also decide to migrate to another site if its body reserves permit it to cover the distance to the destination site. If an individual decides to depart, it should fly to the site yielding the maximum expected fitness at the destination. Once the bird has reached the breeding grounds, its expected reproductive success is determined by time of arrival and body reserves at arrival, assuming that successful breeding is only possible if birds arrive within a rather short time window and that reproductive output is related to the amount of reserves ("capital breeding," for review, see ref. 72). Yet, empirical studies have shown that arctic breeding shorebirds arrive without extensive body fat and are rather "income breeders" (73). Thus, the parameter defining the minimum required body reserves for maximum fitness at optimal arrival was set to 10% of maximum fuel load. The arrival window was set according to the snowmelt date (see below) and used a sigmoidal relation between body reserves upon arrival and expected number of young. When birds failed to reach the breeding grounds within this time window or with insufficient body reserves, they cannot reproduce in the present year but may do so in subsequent year(s). Expected fitness gains from future breeding attempts depend on survival and future reproductive success (for more details on parameters and optimization routine, see *SI Appendix*, sections S1–S3).

**Simulations.** With the dynamic programming equations, we calculated matrices containing the optimal behavioral decisions for all combinations of fuel stores, times and sites and for all three scenarios of past, present and future environmental conditions and for all empirically tracked individuals with their specific start and end point of migration. Furthermore, we used the errors in decision-making approach, which allows deviations from perfectly optimal behavior given such deviations have only little cost (74). Consequently, decisions, i.e., behavioral alternatives, are chosen based on a probability, which depends on its fitness consequences. These probabilities are then used in subsequent forward simulations to follow individual birds during their journeys and to generate predictions of individual migratory behavior, i.e., departure, arrival, and staging times. For each scenario and each empirically observed starting (wintering) and end (breeding) point, we initialized a population of 200 individuals with randomly distributed initial body reserves of $x$ (with $30 < x < 50$) start in the wintering site at $t = 15$ (15th of January). Thereafter, all individuals are assumed to behave nearly optimally according to their present body reserves, site, and time by performing an action, i.e., migrating to site $j$ or staying and foraging with intensity $u$, with probabilities corresponding to their fitness reward. The resulting individual migration tracks were summarized and analyzed in the same way as described for the empirical tracking data.

All analyses were done in R [Version 4.1, R Core Team (75)], with integration of C++ code using the R package Rcpp (76).

**Table 2. Species parameters derived from the literature (body weight BW), allometric relationships (kJ per g of BW, FDR, days to refuel DTR, basal metabolic rate BMR, and conductance Kesm), and empirical tracking (flight range)**

| Species | BW$_{min}$ [g] | BW$_{max}$ [g] | g\|x\|kJ | FDR$_{max}$ [x/d] | DTR [d] | BMR [x/d] | K$_{esm}$ [°C] | Flight range [km] |
|---|---|---|---|---|---|---|---|---|
| Bar-tailed Godwit | 250 | 534 | 1\|2.84\|93.2 | 5.16 | 19.66 | 1.84 | 20.6 | 12.650 |
| Great Knot | 144 | 303 | 1\|1.59\|52.3 | 5.99 | 16.66 | 1.23 | 23.6 | 9.540 |
| Red Knot | 105 | 208 | 1\|1.19\|39.2 | 6.45 | 15.50 | 1.01 | 24.9 | 8.335 |
| Curlew Sandpiper | 55 | 110 | 1\|0.49\|16.1 | 7.98 | 12.52 | 0.56 | 29.2 | 5.700 |
| Red-necked Stint | 23 | 45 | 1\|0.13\|4.5 | 10.22 | 9.78 | 0.29 | 31.2 | 3.800 |

Maximal FDR and DTR correspond to the allometric relationship derived via empirical measurements (summarized in 70) and multiplied by 1.5 (see *Materials and Methods* for details), providing the assumed maximum FDR in optimal (ad libitum) conditions and constant 12 h feeding intensity.

Author affiliations: [a]Alfred Wegener Institute Helmholtz Centre for Polar and Marine Research, Section Polar Terrestrial Environmental Systems, Potsdam 14473, Germany; [b]School of Earth, Atmospheric and Life Sciences, University of Wollongong, Wollongong, NSW 2522, Australia; [c]Conservation Ecology Group, Groningen Institute for Evolutionary Life Sciences, University of Groningen, Groningen 9700, The Netherlands; [d]Zoology and Ecology Group, Massey University, Palmerston North 4442, New Zealand; [e]School of the Environment, The University of Queensland, Brisbane, QLD 4072, Australia; [f]Victorian Wader Study Group, Blackburn, VIC 3130, Australia; [g]Centre for Integrative Ecology, School of Life and Environmental Sciences, Deakin University, VIC 3217, Australia; [h]German Aerospace Center, The Remote Sensing Technology Institute, Berlin 12489, Germany; [i]Department of Remote Sensing, EAGLE M. Sc. Program, University of Würzburg, Würzburg 97074, Germany; [j]College of Science and Engineering, James Cook University, Townsville, QLD 4811, Australia; [k]Federal Research Institute WSL, Birmensdorf 8903, Switzerland; [l]Department of Bird Migration, Swiss Ornithological Institute, Sempach 6204, Switzerland; [m]Institute of Biodiversity and Ecosystem Dynamics, University of Amsterdam, Amsterdam 1090 GE, The Netherlands; and [n]Department of Environmental Systems Science, ETH Zürich, Zürich 8902, Switzerland

1. S. L. Maxwell, R. A. Fuller, T. M. Brooks, J. E. M. Watson, Biodiversity: The ravages of guns, nets and bulldozers. *Nature* **536**, 143–145 (2016).
2. C. A. Runge, T. G. Martin, H. P. Possingham, S. G. Willis, R. A. Fuller, Conserving mobile species. *Front. Ecol. Environ.* **12**, 395–402 (2014).
3. V. Radchuk *et al.*, Adaptive responses of animals to climate change are most likely insufficient. *Nat. Commun.* **10**, 3109 (2019).
4. J. R. Conklin, S. Lisovski, P. F. Battley, Advancement in long-distance bird migration through individual plasticity in departure. *Nat. Commun.* **12**, 4780 (2021).
5. D. S. Wilcove, M. Wikelski, Going, going, gone: Is animal migration disappearing. *PLoS Biol.* **6**, e188 (2008).
6. C. S. Mantyka-pringle, T. G. Martin, J. R. Rhodes, Interactions between climate and habitat loss effects on biodiversity: A systematic review and meta-analysis. *Global Change Biol.* **18**, 1239–1252 (2012).
7. C. Parmesan, Ecological and evolutionary responses to recent climate change. *Annu. Rev. Ecol. Evol. Syst.* **37**, 637–669 (2006).
8. S. J. Thackeray *et al.*, Phenological sensitivity to climate across taxa and trophic levels. *Nature* **535**, 241–245 (2016).
9. C. Both *et al.*, Avian population consequences of climate change are most severe for long-distance migrants in seasonal habitats. *Proc. R Soc. B Biol. Sci.* **277**, 1259–1266 (2009).
10. S. S. Renner, C. M. Zohner, Climate change and phenological mismatch in trophic interactions among plants, insects, and vertebrates. *Ann. Rev. Ecol. Evol. Syst.* **49**, 165–182 (2018).
11. T. P. Weber, A. I. Houston, B. J. Ens, Consequences of habitat loss at migratory stopover sites: A theoretical investigation. *J. Avian Biol.* **30**, 416–426 (1999).
12. T. Iwamura *et al.*, Migratory connectivity magnifies the consequences of habitat loss from sea-level rise for shorebird populations. *Proc. R Soc. B Biol. Sci.* **280**, 20130325 (2013).
13. G.-R. Walther *et al.*, Ecological responses to recent climate change. *Nature* **416**, 389–395 (2002).
14. D. S. Melville, Y. Chen, Z. Ma, Shorebirds along the Yellow Sea coast of China face an uncertain future–A review of threats. *Emu Austral. Ornithol.* **116**, 100–110 (2016).
15. N. J. Murray, R. S. Clemens, S. R. Phinn, H. P. Possingham, R. A. Fuller, Tracking the rapid loss of tidal wetlands in the Yellow Sea. *Front. Ecol. Environ.* **12**, 267–272 (2014).
16. Z. Ma *et al.*, Rethinking China's new great wall. *Science* **346**, 912–914 (2014).
17. R. Clemens *et al.*, Continental-scale decreases in shorebird populations in Australia. *Emu Austral. Ornithol.* **116**, 119–135 (2016).
18. C. E. Studds *et al.*, Rapid population decline in migratory shorebirds relying on Yellow Sea tidal mudflats as stopover sites. *Nat. Commun.* **8**, 14895 (2017).
19. T. Amano, T. Székely, K. Koyama, H. Amano, W. J. Sutherland, A framework for monitoring the status of populations: An example from wader populations in the East Asian-Australasian flyway. *Biol. Conserv.* **143**, 2238–2247 (2010).
20. S. Bauer, B. J. Hoye, Migratory animals couple biodiversity and ecosystem functioning worldwide. *Science* **344**, 1242552 (2014).
21. F. Jeltsch *et al.*, Integrating movement ecology with biodiversity research–exploring new avenues to address spatiotemporal biodiversity dynamics. *Mov. Ecol.* **1**, 6 (2013).
22. C. Both, S. Bouwhuis, C. M. Lessells, M. E. Visser, Climate change and population declines in a long-distance migratory bird. *Nature* **441**, 81–83 (2006).
23. S. Lisovski, K. Gosbell, C. Minton, M. Klaassen, Migration strategy as an indicator of resilience to change in two shorebird species with contrasting population trajectories. *J. Anim. Ecol.* **13393**, 1365–2656 (2020), 10.1111/1365-2656.13393.
24. K. L. Dhanjal-Adams *et al.*, Setting conservation priorities for migratory networks under uncertainty. *Conserv. Biol.* **31**, 646–656 (2017).
25. M. Zhao *et al.*, Body size shapes inter-specific migratory behaviour: Evidence from individual tracks of long-distance migratory shorebirds. *J. Avian Biol.* **49**, jav-01570 (2018).
26. J. Conklin, N. Senner, P. Battley, T. Piersma, Extreme migration and the individual quality spectrum. *J. Avian Biol.* **48**, 19–36 (2017).
27. T. P. Weber, B. J. Ens, A. I. Houston, Optimal avian migration: A dynamic model of fuel stores and site use. *Evolution. Ecol.* **12**, 377–401 (1998).
28. S. Bauer, S. Lisovski, R. J. F. M. Eikelenboom-Kil, M. Shariati, B. A. Nolet, Shooting may aggravate rather than alleviate conflicts between migratory geese and agriculture. *J. Appl. Ecol.* **55**, 2653–2662 (2018).
29. S. Bauer, M. Klaassen, Mechanistic models of animal migration behaviour–Their diversity, structure and use. *J. Anim. Ecol.* **82**, 498–508 (2013).
30. J. A. van Gils *et al.*, Body shrinkage due to Arctic warming reduces red knot fitness in tropical wintering range. *Science* **352**, 819–821 (2016).
31. J. Hartfelder *et al.*, The allometry of movement predicts the connectivity of communities. *Proc. Natl. Acad. Sci. U.S.A.* **117**, 22274–22280 (2020).
32. R. I. Bailey, F. Molleman, C. Vasseur, S. Woas, A. Prinzing, Large body size constrains dispersal assembly of communities even across short distances. *Sci. Rep.* **8**, 10911 (2018).
33. E. Paradis, S. R. Baillie, W. J. Sutherland, R. D. Gregory, Patterns of natal and breeding dispersal in birds. *J. Anim. Ecol.* **67**, 518–536 (1998).
34. T. Piersma, Hop, skip, or jump? Constraints on migration of arctic waders by feeding, fattening, and flight speed. *Limosa* **60**, 185–194 (1987).
35. S. R. Evans, S. Bearhop, Variation in movement strategies: Capital versus income migration. *J. Anim. Ecol.* **91**, 1961–1974 (2022).
36. S. Lisovski, K. Gosbell, C. Hassell, C. Minton, Tracking the full annual-cycle of the Great Knot Calidris tenuirostris, a long-distance migratory shorebird of the East Asian-Australasian Flyway. *Wader Study* **123**, 177–189 (2016).
37. R. E. Gill *et al.*, Extreme endurance flights by landbirds crossing the Pacific Ocean: Ecological corridor rather than barrier? *Proc. R Soc. B Biol. Sci.* **276**, 447–457 (2008).
38. P. F. Battley *et al.*, Contrasting extreme long-distance migration patterns in bar-tailed godwits Limosa lapponica. *J. Avian Biol.* **43**, 21–32 (2012).
39. N. W. Cooper, T. W. Sherry, P. P. Marra, Experimental reduction of winter food decreases body condition and delays migration in a long-distance migratory bird. *Ecology* **96**, 1933–1942 (2015).
40. E. Rakhimberdiev *et al.*, Fuelling conditions at staging sites can mitigate Arctic warming effects in a migratory bird. *Nat. Commun.* **9**, 4263 (2018).
41. C. Both, Flexibility of timing of avian migration to climate change masked by environmental constraints en route. *Curr. Biol.* **20**, 243–248 (2010).
42. C. Both, R. G. Bijlsma, J. Ouwehand, Repeatability in spring arrival dates in pied flycatchers varies among years and sexes. *Ardea* **104**, 3–21 (2016).
43. C. E. Studds, P. P. Marra, Rainfall-induced changes in food availability modify the spring departure programme of a migratory bird. *Proc. R Soc. B Biol. Sci.* **278**, 3437–3443 (2011).
44. W. Cresswell, Migratory connectivity of Palaearctic-African migratory birds and their responses to environmental change: The serial residency hypothesis. *Ibis* **156**, 493–510 (2014).
45. M. A. Verhoeven *et al.*, Generational shift in spring staging site use by a long-distance migratory bird. *Biol. Lett.* **14**, 20170663 (2018).
46. J. A. Gill *et al.*, Why is timing of bird migration advancing when individuals are not? *Proc. R Soc. B Biol. Sci.* **281**, 20132161 (2014).
47. T. K. Lameris *et al.*, Mismatch-induced growth reductions in a clade of Arctic-breeding shorebirds are rarely mitigated by increasing temperatures. *Global Change Biol.* **28**, 829–847 (2022).
48. A. A. Hoffmann, C. M. Sgrò, Climate change and evolutionary adaptation. *Nature* **470**, 479–485 (2011).
49. P. Gienapp, C. Teplitsky, J. S. Alho, J. A. Mills, J. Merilä, Climate change and evolution: Disentangling environmental and genetic responses. *Mol. Ecol.* **17**, 167–178 (2008).
50. C. Howard *et al.*, Explaining and predicting animal migration under global change. *Divers. Distrib.* **30**, e13797 (2024).
51. P. F. Battley, S. Lisovski, J. R. Conklin, Data from "Bar-tailed Godwit geolocator tracking New Zealand 2008-2014." Movebank Data Repository. https://doi.org/10.5441/001.1.327. Deposited 1 April 2024.
52. P. F. Battley, S. Lisovski, Data from "Red Knot geolocator tracking New Zealand 2013." Movebank Data Repository. https://doi.org/10.5441/001.1.328. Deposited 1 April 2024.
53. S. Lisovski, K. Gosbell, C. Minton, M. Klaassen, Data from "Migration strategy as an indicator of resilience to change in two shorebird species with contrasting population trajectories [curlew sandpipers]." Movebank Data Repository. https://doi.org/10.5441/001.1.g2n3ps20. Deposited 24 November 2020.
54. S. Lisovski, K. Gosbell, C. Minton, M. Klaassen, Data from "Migration strategy as an indicator of resilience to change in two shorebird species with contrasting population trajectories [red-necked stints]." Movebank Data Repository. https://doi.org/10.5441/001.1.s07tk38d. Deposited 24 November 2020.
55. S. Lisovski *et al.*, Light-level geolocator analyses: A user's guide. *J. Anim. Ecol.* **89**, 221–236 (2020).
56. E. Rakhimberdiev *et al.*, Comparing inferences of solar geolocation data against high-precision GPS data: Annual movements of a double-tagged black-tailed godwit. *J. Avian Biol.* **47**, 589–596 (2016).

57. S. Bauer, B. J. Ens, M. Klaassen, Many routes lead to Rome: potential causes for the multi-route migration system of Red Knots, *Calidris canutus islandica*. *Ecology* **91**, 1822–1831 (2010).

58. S. Bauer, M. Van Dinther, K.-A. Høgda, M. Klaassen, J. Madsen, The consequences of climate-driven stop-over sites changes on migration schedules and fitness of Arctic geese. *J. Anim. Ecol.* **77**, 654–660 (2008).

59. E. Kalnay *et al.*, The NCEP/NCAR 40-year reanalysis project. *Bull. Am. Meteorol. Soc.* **77**, 437–472 (1996).

60. T. Semmler *et al.*, Simulations for CMIP6 with the AWI climate model AWI-CM-1-1. *J. Adv. Model. Earth Syst.* **12**, e2019MS002009 (2020).

61. N. J. Murray *et al.*, The global distribution and trajectory of tidal flats. *Nature* **565**, 222–225 (2019).

62. C. Giri *et al.*, Status and distribution of mangrove forests of the world using earth observation satellite data. *Global Ecol. Biogeograp.* **20**, 154–159 (2011).

63. J. R. Conklin, Y. I. Verkuil, B. Smith, Prioritizing migratory shorebirds for conservation action on the East Asian-Australasian Flyway (WWF Hong Kong, 2014).

64. D. A. Robinson, T. W. Estilow, N.C.D.R. Program, NOAA Climate Date Record (CDR) of Northern Hemisphere (NH) Snow Cover Extent (SCE). NOAA National Centers for Environmental Information (2012). doi:https://doi.org/10.7289/V5N014G9. Accessed 15 December 2020.

65. U. G. von Blotzheim, *Handbuch der Vögel Mitteleuropas Band 8 I Teil Charadriiformes 3.Teil* (Akademische Verlagsgesellschaft, 1982).

66. Å. Lindström, Maximum fat deposition rates in migrating birds. *Ornis Scandinavica (Scandinavian J. Ornithol.)* **22**, 12–19 (1991).

67. Y. Aharon-Rotman, K. Gosbell, C. Minton, M. Klaassen, Why fly the extra mile? Latitudinal trend in migratory fuel deposition rate as driver of trans-equatorial long-distance migration. *Ecol. Evol.* **6**, 6616–6624 (2016).

68. M. Kersten, T. Piersma, High levels of energy expenditure in shorebirds; metabolic adaptations to an energetically expensive way of life. *Ardea* **55**, 175–187 (1987).

69. C. J. Pennycuick, S. Åkesson, A. Hedenström, Air speeds of migrating birds observed by ornithodolite and compared with predictions from flight theory. *J. R Soc. Interface* **10**, 20130419 (2013).

70. A. Kvist, Å. Lindström, M. Green, T. Piersma, G. H. Visser, Carrying large fuel loads during sustained bird flight is cheaper than expected. *Nature* **413**, 730–732 (2001).

71. J. M. McNamara, A. I. Houston, S. L. Lima, Foraging routines of small birds in winter: A theoretical investigation. *J. Avian Biol.* **25**, 287–302 (1994).

72. P. A. Stephens, I. L. Boyd, J. M. McNamara, A. I. Houston, Capital breeding and income breeding: Their meaning, measurement, and worth. *Ecology* **90**, 2057–2067 (2009).

73. M. Klaassen, Å. Lindström, H. Meltofte, T. Piersma, Arctic waders are not capital breeders. *Nature* **413**, 794–794 (2001).

74. J. M. McNamara, J. N. Webb, E. J. Collins, T. Székely, A. I. Houston, A general technique for computing evolutionarily stable strategies based on errors in decision-making. *J. Theor. Biol.* **189**, 211–225 (1997).

75. R Core Team, *R: A Language and Environment for Statistical Computing* (R Foundation for Statistical Computing, 2018).

76. D. Eddelbuettel, J. J. Balamuta, Extending R with C++: A Brief Introduction to Rcpp. *Am. Stat.* **72**, 28–36 (2018).